Ultrasound in Med. & Biol., Vol. 37, No. 1, pp. 59–68, 2011

0301-5629/$ - see front matter

ELSEVIER

doi:10.1016/j.ultrasmedbio.2010.10.013

● *Original Contribution*

IMAGING OF THE OVINE CORPUS LUTEUM MICROCIRCULATION WITH CONTRAST ULTRASOUND

VASSILIS SBOROS,* M. AVERKIOU,† M. LAMPASKIS,† D. H. THOMAS,* N. SILVA,* C. STROUTHOS,† J. DOCHERTY,‡ and A. S. MCNEILLY‡

*Medical Physics and Centre for Cardiovascular Sciences, Queens Medical Research Institute, University of Edinburgh, Edinburgh, UK; †Department of Mechanical and Manufacturing Engineering, University of Cyprus, Nicosia, Cyprus; and ‡Medical Research Council Human Reproductive Sciences Unit, Queens Medical Research Institute, University of Edinburgh, Edinburgh, UK

(*Received* 3 *November* 2009; *revised* 21 *September* 2010; *in final form* 9 *October* 2010)

Abstract—Ultrasound contrast agents have been the subject of microvascular imaging research. The sheep corpus luteum (CL) is a microvascular tissue that provides a natural angiogenic and antiangiogenic process, which changes during the luteal phase of the estrous cycle of the ewe. It can also be controlled and monitored endocrinologically, providing a very attractive *in vivo* model for the study and development of microvascular measurement. The perfusion of the fully developed CL between days 8 and 12 of the estrous cycle was studied in six ewes. A Philips iU22 ultrasound scanner (Bothell, WA, USA) with the linear array probe L9-3 was used to capture contrast-enhanced images after an intravenous bolus injection of 2.4 mL SonoVue (Bracco S.P.A., Milan, Italy). Time-intensity curves of a region of interest inside the CL were formed from linearized image data. A lagged-normal model to simulate the compartmental kinetics of the microvascular flow was used to fit the data, and the wash-in time was measured. Good contrast enhancement was observed in the CLs of all animals and the wash-in time averaged at 5.5 s with 9% uncertainty. The regression coefficient was highly significant for all fits. These data correlated with stained endothelial area in the histology performed postmortem. Two ewes were injected with prostaglandin F2alpha to induce CL regression, which resulted in an increase of wash-in time after a few hours. The CL of the ewe is thus proposed as an ideal model for the study and development of microvascular measurements using contrast ultrasound. Our initial results demonstrate a highly reproducible model for the study of the microvascular hemodynamics in a range of tissues and organs. (E-mail: Vassilis.Sboros@ed.ac.uk) © **2011 World Federation for Ultrasound in Medicine & Biology.**

Key Words: **Sheep ovary, Microbubble, SonoVue, Ultrasound, Tracer kinetics, Contrast imaging.**

INTRODUCTION

Ultrasound imaging is a widely used diagnostic tool and, with the introduction of microbubble (MB) contrast agents, it provides an enhanced capability to visualize the vascular space. Imaging of microvascular flow and perfusion have thus been the subject of ultrasound contrast techniques for nearly 20 years (Sboros and Tang 2010), because they would be of diagnostic value to a wide range of diseases. Today, a number of techniques that look into the microvascular space are slowly being adopted in the clinic, mainly in cardiology (Kaufmann et al. 2007) and liver radiology (Quaia 2007; Averkiou et al. 2010). However, a number of problems remain unresolved and an objective quantification method is yet to be established. In cardiology, for example, apical sections of the myocardium compare better than other sections with single photon emission computed tomography as the gold standard (Gudmundsson et al. 2010), which is perhaps related to the unresolved ventricular nonlinear attenuation (Tang and Eckersley 2006). Both the myocardium and the liver, as well as the large number of other organs that have been investigated, offer complex vascularities and challenges for contrast-enhanced ultrasound (CEUS). Current transducer and signal processing technologies have offered excellent tissue cancellation and today "contrast-only" images are commonplace.

Ultrasound contrast MBs remain in the vascular space (Jayaweera et al. 1994; Lindner et al. 2002), unlike other

Address correspondence to: Vassilis Sboros, Medical Physics, School of Clinical Sciences and Community Health, The University of Edinburgh, The Chancellor's Building, 49 Little France Crescent, Edinburgh, EH16 4SB, UK. E-mail: Vassilis.Sboros@ed.ac.uk

imaging modalities' contrast materials. Although MB kinetics cannot thus offer a true representation of perfusion, which incorporates permeability and nutrient delivery, it offers the advantage of simplicity. With the available evidence, the measurement of microvascular or capillary blood flow and volume should be attainable for CEUS. However, the uncertainties of such measurements remain high, and quantification of microvascular flow is yet to be achieved (Sboros and Tang 2010). Microbubbles combined with ultrasound offer a number of engineering challenges, and CEUS can be further improved. In addition, the literature on the quantification of microvascular flow and volume is limited (Sboros and Tang 2010). A number of kinetics models have been proposed for destruction replenishment or bolus studies (Strouthos et al. 2010), but to our knowledge there are no *in vivo* tissue models that may aid in their development. In general, the development of CEUS has been attempting complex measurements, under elaborate experimental conditions and in challenging microvascular systems such as the myocardium and the liver. The present communication proposes the ovine ovarian corpus luteum (CL) as one such model.

Briefly, both the ovary and endometrium undergo regulated cyclic angiogenesis and vascular regression during the estrus cycle. The changes in, and regulation of, ovarian angiogenesis is an active research field (McNeilly and Fraser 1987; McNeilly et al. 1992b; Fraser and Lunn 2000; Fraser et al. 2000; Wulff et al. 2002; Souza et al. 2003, 2004) in relation to both maximizing fertility and potential treatments of reproductive pathologies that feature microvascular growth or regression (Fraser and Duncan 2009). Although the outer layer of thecal cells of the follicle has a minor vascular supply, the inner granulosa cell layer of the preovulatory follicle, separated by a basement membrane from the thecal layer, is avascular. At the time of ovulation, when the preovulatory follicle releases the oocyte, the follicle collapses and there is a marked and predictable vascularization of these steroidogenic granulosa cells. The resulting CL has a highly developed microvascular network to the extent that each steroidogenic cell is adjacent to, or very close to, an endothelial cell and the CL has a blood supply, per unit mass, eight times that of the kidney. In the absence of pregnancy, a regression of vasculature occurs and in a matter of days, the CL becomes an avascular remnant. Various hormones including the locally acting vascular endothelial growth factor (VEGF) have a role in the CL development (Fraser and Lunn 2000; Dickson et al. 2001; Wulff et al. 2001a, 2001b, 2002; Yong et al. 2003; Fraser et al. 2005). Thus, the CL provides a natural angiogenic and anti-angiogenic regulation with well-established endocrinologic monitoring, and in the sheep it can be controlled by hormone or similar treatments. It can thus be used to develop quantitative methodologies that may be of use to all microvascular imaging studies.

Contrast-enhanced ultrasound has been used to investigate ovarian pathology, with the main focus being cancer (Orden et al. 2003; Kohzuki et al. 2005; Testa et al. 2007). One study on the normal cycle of the sheep ovary, measuring contrast kinetics in the whole ovary (*i.e.*, including CL and all other vasculature), provided significant differences between the follicular and the luteal phase (Marret et al. 2006). In view of the large vascular heterogeneity of the ovary, these authors proposed selective sampling of regions for contrast analysis to improve on vascular discrimination within any lesion (Orden et al. 2003). In addition to this, as mentioned before, the CL offers a unique opportunity for a model system that is central to an investigation on the quantification of microvascular flow. To our knowledge, such an experimental *in vivo* model has not been reported previously and in the present communication, we aim to establish this *in vivo* model for the development of microvascular imaging using CEUS. Real-time imaging of the microvascular blood flow of the CL with low mechanical index (MI) was adopted. To achieve our aim, a quantification scheme for the extraction of hemodynamic-related parameters followed. The experimental uncertainty, as well as comparison with the gold standard of histology, is presented. The potential use of the CL model to simulate vascular regression is explored.

MATERIALS AND METHODS

Animal protocol

These studies were performed at the MRC Human Reproductive Sciences Unit (Edinburgh, UK), and all animal procedures were approved and conducted in accordance with the Home Office Animals (Scientific Procedures) Act 1996 of the United Kingdom. Six Scottish black-face ewes (age, 4 to 5 y; body weight, 55 to 66 kg) exhibiting normal reproductive cycles and having had at least two successful pregnancies were used in this study. The perfusion of fully functional CL was studied on days 8–12 of the estrous cycle in six sheep. In November, which is within the fertile season for the sheep, progestogen-impregnated sponges (60 mg medroxy-progesterone acetate pre-sponge; Intervet Laboratories Ltd., Cambridge, UK) were inserted in all animals. After 14 d *in situ*, sponges were withdrawn, and on day 12 of the subsequent estrous cycle, luteal regression was induced by prostaglandin F2alpha (100 μg intramuscular cloprostenol; Estrumate; Coopers Animal Health, Crewe, Cheshire, UK). Progesterone was measured in blood samples from each ewe taken on day 6 of this second estrous cycle and assayed by nonextraction radioimmunoassay (sensitivity 0.2 ng/mL; intra-assay

CV = 7%) to ensure that a functional CL was present (plasma progesterone >4 ng/mL) (McNeilly et al. 1992a). This process ensured a reproducible and time-controlled estrous cycle that may be studied experimentally, and the age of the CL to be studied is known accurately in each animal. On the day of experiment, a jugular cannula was inserted before each ewe was anesthetized and subsequently maintained under general anesthesia throughout the rest of the study. The ovaries were exposed through midline abdominal incision and one ovary containing a fully functional CL, assessed from the progesterone previously assayed, and healthy appearance, was positioned carefully subcutaneously and held in position with forceps on the ligament so that the blood supply was not affected. The ovary was then covered in ultrasound gel (Henleys Medical, Wellwyn Garden City, Herts, UK), the ultrasound probe placed directly over the corpus luteum and held in place with an adjustable clamp attached to the operating table as described in detail here later. At the end of the experiment, the ewes were killed with an overdose of sodium pentobarbitone (Euthetal; Rhone-Merieux Ltd., Harlow, UK), the scanned ovary removed, the CL cut in the plane of the scan, the whole ovary fixed in Bouins for 6 h and then transferred to 70% alcohol before processing for immunohistochemistry.

In addition to the aforementioned to assess the usefulness of this animal model as a model of vascular regulation, we performed a pilot study to follow the changes in the microvasculature after induction of CL regression and decline in progesterone secretion after injection of prostaglandin F2alpha in two sheep (McNeilly et al. 1992b).

Histochemical visualization of the CL microvasculature

The vasculature of each CL was visualized by detection of lectin BS-1 (from *Bandeiraea simplicifolia*) binding to endothelial cells (Redmer et al. 2001). After fixation and dehydration, sheep ovaries were embedded in paraffin wax. Each CL was sectioned at 5-μm thickness, and each tenth section stained for endothelial cells using lectin from *Bandeiraea simplicifolia* (BS-1; Sigma, UK). Sections were dewaxed in xylene and rehydrated in decreasing concentrations of alcohol (100, 90 and 75%). Antigen retrieval was performed by pressure-cooking the sections in citrate buffer (0.01 M) pH 6.0 for 5 min at full pressure. After a 5-min wash in water and another in 0.1-M phosphate-buffered saline (PBS), sections were blocked in 3% H_2O_2 in methanol for 30 min to inhibit endogenous peroxidase activity. After another wash in water (5 min) and PBS (2 × 5 min), combined avidin-biotin block was performed according to the manufacturer's instructions (Vector Laboratories, Peterborough, UK). Nonspecific background was blocked for 30 min at room temperature with 10% normal goat serum (NGS; Diagnostics Scotland, Carluke, UK) diluted 1:5 in PBS containing 5% bovine serum albumin. To localize endothelial cells, slides were incubated at 4°C overnight in a humidity chamber with a biotin-conjugated lectin from *Bandeiraea simplicifolia* (BS-1; Sigma) diluted 1:80 in PBS. Negative controls were performed by replacing BS-1 with normal goat serum. After washing in PBS (2 × 5 min), slides were incubated in streptavidin horseradish peroxidase (Vector Laboratories) diluted 1:1000 in PBS for 30 min. Bound lectin was visualized using 3,3′-diaminobenzidine tetrahydrochloride (Dako Corp., Glostrup, Denmark). Sections were counterstained with hematoxylin, dehydrated, mounted and visualized by light microscopy. The section of CL with the maximum diameter was equivalent to the region where the scans had been quantified. This was identified and the three sections either side (total $n = 7$) were analyzed. To measure the area of the vascular bed of these sections, the entire cross-sectional area of each section was photographed by tiling 20 images, and the area of staining identified and measured in Photoshop (Adobe Systems, San Jose, CA, USA) (Fraser et al. 2000). A mean area of the vascular bed in the area where the scans were taken was thus generated for each CL.

Imaging and quantification protocol

All CEUS examinations were performed on a Philips iU22 ultrasound scanner (Philips Medical Systems, Bothell, WA, USA) with the linear array probe L9-3. The imaging parameters were: power modulation transmit frequency 3.1 MHz at low transmit power to avoid bubble destruction (MI, 0.05) at 12 fps and one focus below the level of the CL to ensure a uniform acoustic field. The contrast-processed image was displayed side by side with the standard grey-scale image, which is termed *Contrast Side/Side* on the specific scanner we used. Image loops of 60 s were acquired and the linear image data were saved (the logarithmic compression of the machine was removed). The dynamic range was 38 dB for the contrast image. The contrast injection consisted of an intravenous bolus of 2.4 mL of contrast agent (SonoVue, Bracco S.P.A., Milan, Italy) injected into the jugular vein catheter followed by a saline flush of 10 mL, which ensured that all the contrast in the line was administered to the animal. SonoVue is a flexible phospholipid shelled and has a sulfur hexafluoride gas core. The durations of the bolus release were 1 and 3 s, respectively for contrast and saline, and effort was placed to have a reproducible bolus administration.

To position the ultrasound probe, the ultrasonographer found the required image plane using B-mode imaging (conventional noncontrast-specific). The ultrasound probe was clamped onto a manipulator (UM-3C,

Narishige, Kyoto, Japan) that allowed movement in three axes. Small adjustments were made to find the optimal plane of the CL to image. The optimal plane was considered to be the one where the largest area of the CL could be seen. It was assumed that the imaged plane coincided with the center of the CL because it is approximately spherical in shape. Because the experiments could last several hours, small adjustments were performed to maintain the same plane for that period.

Image analysis

The initial image analysis and quantification were carried out using the commercial quantification software (Q-LAB v6, Philips Healthcare, Andover, MA, USA). The tasks included segmentation of the CL (*i.e.*, selection of a region of interest [ROI] for analysis) and formulation of time-intensity curves for that ROI. The logarithmic compression of the ultrasound scanner was removed to restore the data to a linear scale referred to as "linearized" data (Averkiou et al. 2010; Lampaskis et al. 2010). The scanner provides information on the compression that the Q-LAB software can use to uncompress the data to their original linear scale. This has also been tested with an *in vitro* phantom by the authors to establish the linearity of the data (Lampaskis et al. 2010). The measurement of intensity of the selected ROI for all the frames within a loop as a function of time provides the time-intensity curve for a loop. The small movement of the CL during breathing was almost exclusively in plane, as visualized, and motion compensation was performed (Averkiou et al. 2010), ensuring that the same ROI was maintained throughout the time-intensity curve. Typical images from a loop capture are displayed in Fig. 1, also demonstrating the Contrast Side/Side display. The left column (a, c) are "contrast-only" or "vascular-only" images, whereas the right column (b, d) are the conventional (fundamental) grey-scale images. The ROIs containing the CL were selected based on the contrast (Fig. 1a) at peak intensity and also later during the washout of the contrast agent (Fig. 1c). The intention in the ROI selection was to include only the microvascular network of the CL and not the larger macrovessels. As shown in Fig. 2a (which may also include an artifact known as "blooming"), a considerable amount of vasculature lies in the outer CL, confirmed by the histological inspection of the tissues postmortem. In the contrast loops, these larger vessels can be judged by their denser and faster contrast kinetics compared with the central CL.

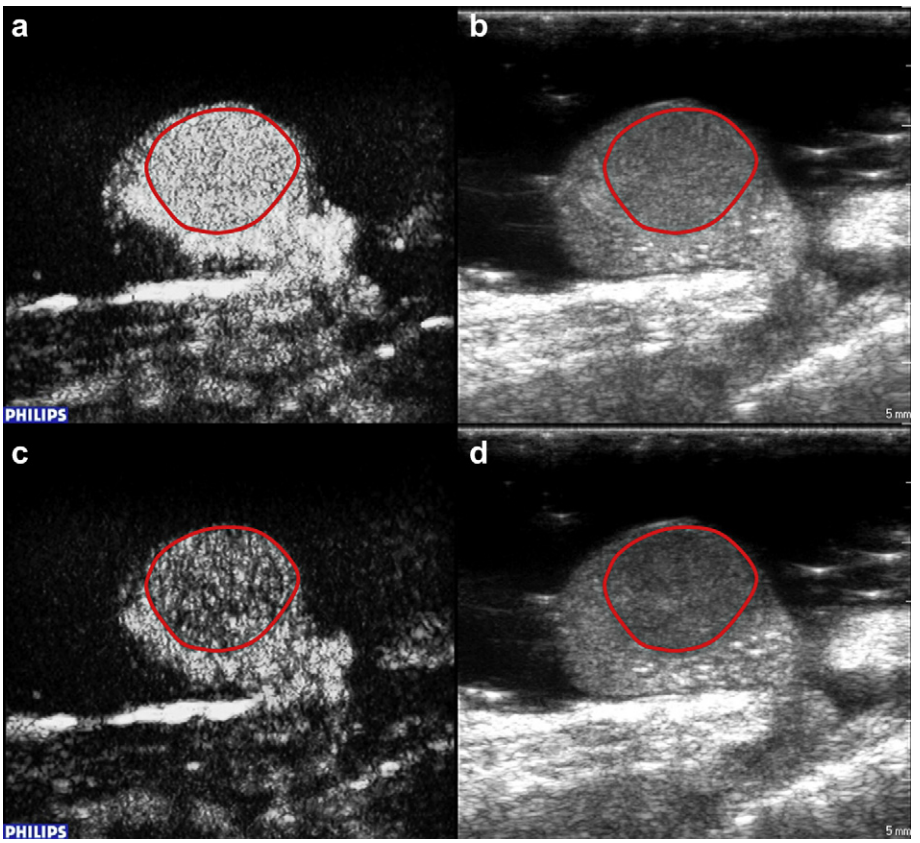

Fig. 1. CEUS image of a fully developed CL at peak enhancement (a), after peak enhancement during washout phase (c) and the corresponding tissue images (b) and (d).

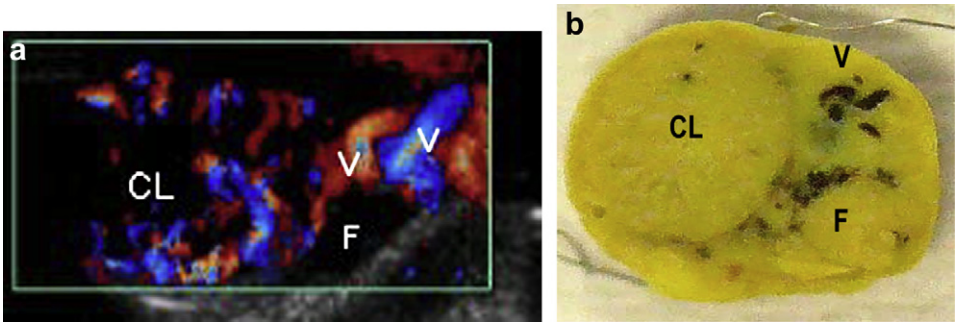

Fig. 2. (a) Color flow Doppler ultrasound scan of a sheep ovary at day 14 of the luteal phase. Larger twisting vessels such as the main arteries and veins (V) as well as their subsequent feeding branches of the CL are possible to distinguish around it. Avascular follicles (F) have no flow and are anechoic. The microvascular flow of the center of the CL cannot be observed. The image has been produced after the washout of a contrast bolus injection, providing slight enhancement of the Doppler images. (b) Photo of a section of the same CL postmortem. The blood was trapped by clamping the ovarian artery upon collection of the tissue. It was then stored in Bouin's fixative, which darkened the blood in the main vessels (under V). The large follicle (F) and the CL (around 1.5 cm in diameter) can also be seen. Sparse dark areas around the CL demonstrate the existence of larger vessels.

A schematic diagram of a typical time-intensity curve produced by our ROI analysis is displayed in Fig. 3. The vertical axis is the image intensity in the ROI, measured in linear arbitrary intensity units. In this plot, the important hemodynamic-related parameters (Strouthos et al. 2010), namely the area under the curve (AUC), the time to peak intensity t_p, the peak intensity I_p and the mean transit time (MTT) are indicated. The MTT is proportional to microvascular volume, whereas the AUC is proportional to volume flow and inversely proportional to volume (Strouthos et al. 2010). A lagged normal model was implemented to simulate the compartmental kinetics of the microvascular flow (Lassau et al. 2007; Averkiou et al. 2010; Strouthos et al. 2010). The measurement of intensity of contrast throughout the 60-s loop was fitted to this model and the wash-in time (WIT) was measured. Although there are a number of parameters that may be measured from such curves (Arditi et al. 2006; Correas et al. 2006; Lassau et al. 2007; Averkiou et al. 2010), we have concentrated only on WIT in the present initial study because it is suggested in the literature to be the most reproducible one (Averkiou et al. 2010; Strouthos et al. 2010). Optimization and adjustment of scanner settings, including gain, focus, depth and compression, was prioritized throughout this study to obtain good constant 2-D plane acquisition and produce data that may be used to fit the compartmental kinetics model. Emphasis was placed on setting the scanner parameters such that signal saturation was avoided so that the "linearized" data would be very close to the raw linear data that are not available in clinical grade ultrasound scanners.

RESULTS

A typical enhancement pattern after a SonoVue (Bracco S.P.A.) bolus injection into a mature CL is shown in Fig. 4. All fully developed CL imaged exhibited significant enhancement after injection of the contrast agent. The contrast agent arrives from larger feeding vessels (contrast area to the top right of the drawn ROI in Fig. 4a) that can be identified in most cases. The ROI in the CL subsequently has a rapid increase in average intensity (Fig. 4 [b, c]). Finally, the contrast intensity within the ROI starts to decrease after several seconds during the washout phase of the bolus (Fig. 4d) and eventually ends in the original background noise levels (Fig. 4e). Figure 4f shows the time-intensity curve, which is the contrast intensity over the CL as a function of time after injection. In some animals, a small area with no enhancement can be seen in the center of the CL, also at the center of the ROI in Fig. 4. This is in agreement with lectin histochemical analysis of the microvasculature and larger blood vessels that also show a cystic area in the center without any microvessels present (Fig. 4 [g, h]). The pattern of microvasculature seen in both the active and regressed CLs is similar to that previously reported (Vonnahme et al. 2006).

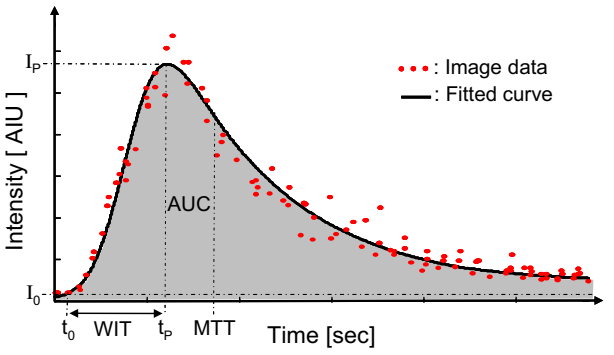

Fig. 3. Schematic diagram of a time-intensity curve. Notice the peak (I_P) and baseline (I_0) intensity, the take off (t_0) and peak (t_P) time, the WIT, the MTT and the AUC.

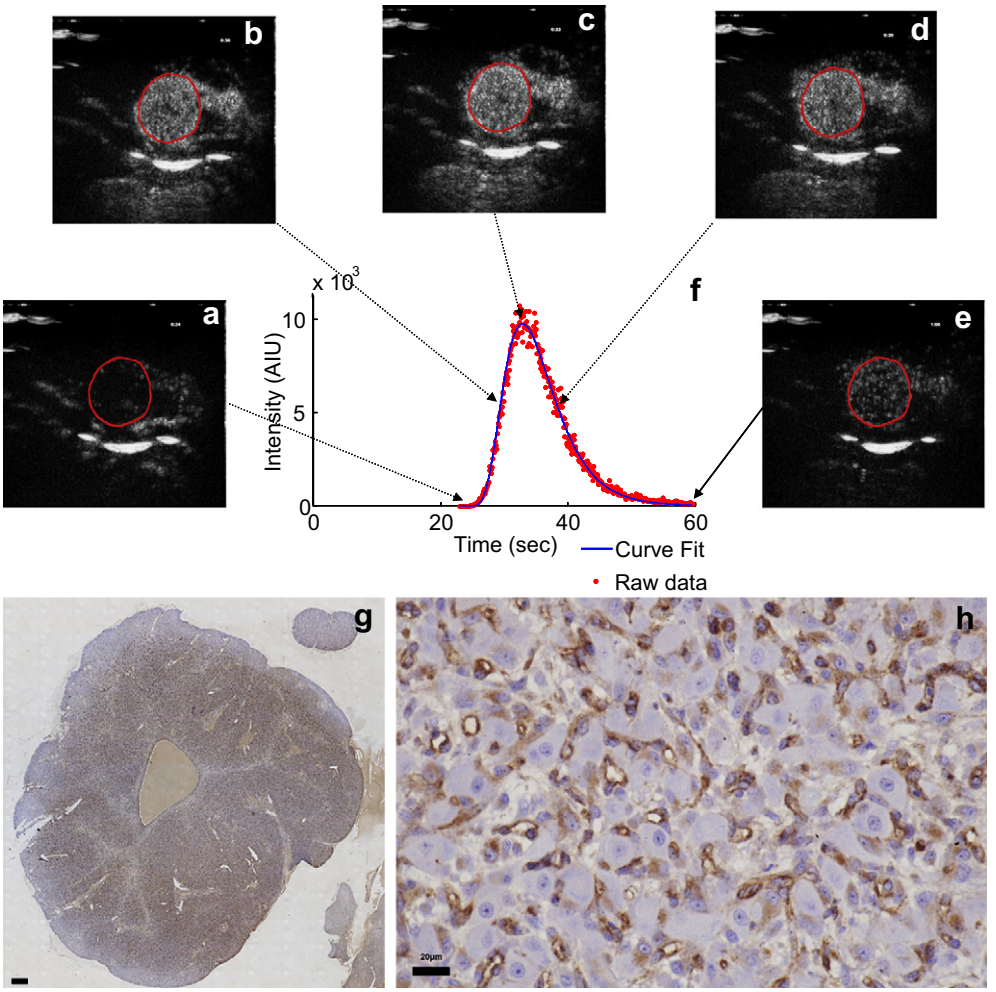

Fig. 4. A typical contrast loop of a fully developed CL (day 9 of estrous cycle) over the transit of the injected bolus (a–e) depicted with the corresponding time-intensity curve (f). Eight loops were captured in the course of 2 h. The data are fitted with the lagged normal model. The WIT was 6.42 ± 0.38 s. Notice the small area in the center with no enhancement in (c) and (d), which corresponds to the cavity in the CL, as seen in (g). Immunohistochemical staining for lectin-identifying endothelial cells of the microvascular bed in the same plane of the CL imaged in (a–e). (g: x20, bar = 250 μm) and (h: x40; bar = 20 μm).

The results from the six animals between days 8 and 12 of the estrous cycle that were studied are summarized in Table 1. The WIT averaged at 5.47 s and the within-animal measurement uncertainty averaged at 9%. The difference between the CL in this group was insignificant. Moreover, five of six animals displayed uncertainty below 9% (averaging at 6%). The animal (R1) with 23% uncertainty was the first in the investigation and the quality of data in terms of image plane stability and good location of a central slice of the CL were problematic. Moreover, the gain and resolution settings were further adjusted to achieve the optimal contrast sensitivity to be used for the subsequent animals. The regression coefficient of the fit was 0.97 or greater for all the data. Again the first animal provided the lowest regression, but still highly significant to the fit. Finally, the WIT uncertainty between animals was 16%, which indicates a low variation between ovarian WIT between days 8 and 12 of the estrous cycle. Four of the animals were immediately killed to compare histological data with WIT. The last column in Table 1 displays the area of vascular endothelium of the central slice of the ultrasound image plane. A significant correlation of 0.98 with the WIT is observed.

The other two animals, R50 and Y50, were given a prostaglandin injection to induce luteolysis and were killed after 8 and 6 h, respectively, which is the time that the vascular area measurement in Table 1 refers to. Figure 5 provides the WIT as it progresses after prostaglandin injection, showing a significant increase of WIT for both cases. The stained area was 3.29 and 3.79 mm^2 for R50 and Y50, respectively. The histological data

Table 1. Summary of time-intensity analysis of contrast images of the ewe CL

Sheep ID/Cycle day	Mean WIT (s)	WIT SD (s)/% uncertainty	R^2	Stained area (mm^2)
R1/8	4.91	1.12/0.23	0.97	5.10
Y169/8	5.06	0.38/0.07	0.98	5.69
B196/8 (also in Fig. 4)	6.42	0.38/0.06	0.99	7.32
R50/11	5.43	0.18/0.03	0.98	3.29*
Y50/11	5.56	0.46/0.08	0.99	3.79*
B197/12	4.18	0.38/0.09	0.99	4.56
Mean mature CL	5.47	0.48/0.09		

Last column provides area of stained endothelium immediately after the ultrasound measurements except in two cases (*), which happened for R50 and for Y50 in 8 and 6 h, respectively, after prostaglandin injection.

cannot be available before prostaglandin injection, and a comparison with the other four CL is only possible.

DISCUSSION

Ultrasound contrast imaging research has aimed at the measurement of microvascular blood flow in various organs and in pathology over the last 20 years. The progress may appear slow and it may be attributed to the complexity that MBs tender as contrast materials, and the parallel evolution in transducer and signal processing technologies. Liver and heart pathology have provided numerous investigations and now offer some new tools that are useful to clinicians (Kaufmann et al. 2007; Quaia 2007; Sboros and Tang 2010). Robust tools for the quantitation of contrast images are not fully developed, however. It is accepted that single MBs can be detected (Sboros et al. 2002a; Klibanov et al. 2002; Sboros et al. 2003), and the technology has matured to achieve high sensitivity at even very low acoustic pressures (Lampaskis et al. 2010), also used in the present study. It is thus becoming more apparent that *in vivo* research in the pursuit of accurate information on microvascularity has a rather unsystematic character. To our knowledge, an *in vivo* model of "controlled" progression and regression of angiogenesis for the development of microvascular imaging is not available in the field of ultrasound.

The current communication provides substantial and encouraging data for a model for microvascular imaging development. As a first step in developing a vascular regulation monitoring model, we have completed the following: (a) successfully imaged the microvascular network of the CL with CEUS, (b) quantified histologically the same microvasculature and (c) quantified the time-intensity curves and fitted them to a model for hemodynamic parameter extraction. The WIT analysis provided a low uncertainty comparable or better with any other available in the literature (Averkiou et al. 2010). The animals that were monitored for several hours after prostaglandin injection provided a number of measurements with uncertainties higher than 10%, because of difficulty in maintaining the constancy of all image parameters. The deviation between different measurements in this initial set of data lends itself to further improvement. A systematic comparison between quantitative immunohistochemical analysis of the CL and the ultrasound data is required in the future to establish the value of such measurements. Also, it is known that local microvascular changes occur within less than an hour as a result of local endocrine regulation within the CL (McNeilly et al. 1992a). On the other hand, maintaining the same plane of view was successfully achieved in this study, though it was more challenging in the longer experiments, which probably was essential in achieving such low variation between different measurements. A systematic approach on the injection contribution is also required, because it has been demonstrated that the injection method may significantly affect the contrast enhancement (Talu et al. 2008).

Although a consistently similar bolus rate was attempted, it is desirable in the future to either use a bolus injector or assess the impact of the bolus in another larger vessel. Precise knowledge of the injected material and low noise intensity data (*i.e.*, that provide highly significant model fits) will further improve the application of indicator dilution models such as the lagged normal model we have used here.

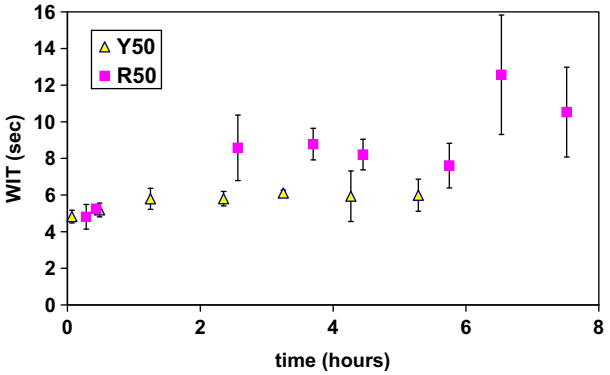

Fig. 5. Progression of WIT with time after prostaglandin injection (time = 0).

A number of compartmental kinetics models have been proposed in the literature with different sets of assumptions (Strouthos et al. 2010). We used a lagged-normal function that assumes a Gaussian-shaped bolus that enters a microvascular volume in a homogeneous and well-mixed fashion (Fisher et al. 2002). Here, the correlation between WIT and stained area in the mature CL confirmed that the MTT (and subsequently the WIT) is proportional to vascular volume (Strouthos et al. 2010). In addition, the low uncertainty of the WIT puts forward a strong case that small microvascular changes of the CL are possible to measure with CEUS. However, in the two prostaglandin-injected animals, the WIT shows an increase with a reduction of vascular volume, because in the first few hours after prostaglandin injection, the CL undergoes vasoconstriction before endothelial cell apoptosis (Ohtani et al. 2004). This is seemingly contrary to the compartmental kinetics models (Strouthos et al. 2010). This relationship, however, assumes conservation of mass that may not be possible with the increased vascular resistance that a reduced vascular volume may offer. The immunohistochemistry result, on the other hand, is not statistically interpretable, because of the low number of animals. The evaluation of CL flow kinetics and related models will be the subject of future work, where it is possible to assess a number of parameters including those related to intensity.

The gold standard of endothelial cell area as a measure of microvascular volume may also not be optimal. It is difficult to accurately provide histological data on the same slice of tissue that was scanned by the ultrasound field or the slice from which the MB response was collected. There are also some fundamental concerns on such data. Although the endothelial cell area is related to vascular lumen cross section, the relationship is difficult to pin down. Further complexities are introduced when the tissue is excised and fixed, which would alter its mechanical state compared with that during the ultrasound measurements. These measurements remain the gold standard in the absence of other measurements, but should be used with caution. We thus avoided attempting a more detailed statistical analysis here.

In addition, there are other important problems in quantitative analysis of MB scatter. Here, we attempted to use scanner settings and MB concentrations that provide intensity values that lie within the linear relationship domain of concentration *vs.* intensity (Lampaskis et al. 2010). *In vitro* experiments show that attenuation, nonlinear propagation, MB destruction and possibly other effects may distort the scatter response from MBs (Sboros et al. 2000, 2001, 2002b; Tang et al. 2005; Tang and Eckersley 2006, 2007). An ROI, such as the one used here, is in fact a 3-D volume exposed to ultrasound of variable frequency content and acoustic pressure amplitudes from zero to a peak value. Further, MBs do not provide Gaussian dispersions of acoustic responses (Sboros et al. 2001, 2002b, 2003), thus producing variable results to pulse sequences (Thomas et al. 2009a). For lipid MBs, this dispersion may be attributed to resonant and nonresonant populations (Thomas et al. 2009b). It is thus evident that the MB dispersion of physical characteristics, including size and shell, is important in the wide dispersion of acoustic responses and may explain the currently suboptimal microvascular assessment using CEUS. With the aid of a research ultrasound scanner, the current *in vivo* setup may be used to test new contrast administration (*e.g.*, monodisperse bubbles) and signal processing protocols.

Further work is required to establish the CL model for monitoring changes in angiogenesis and vascular regression. However, it has been established for a number of years that in sheep the natural prostaglandin F2alpha is the causal agent released by the nonpregnant uterus, which causes the CL to regress (Baird and McNeilly 1981; Baird et al. 1981). This is associated with a loss of endothelial cells over a 24-h period (Vonnahme et al. 2006), but this occurs after the decline in progesterone secretion, which is the functional secretion for the CL. Changes within the structure and/or permeability of the microvasculature may occur, but this is yet to be investigated. Neutralization of VEGF with a VEGF trap also causes a rapid decline in progesterone secretion in the primate CL before any visible change in the microvasculature bed assessed by histology of the CLs (Dickson et al. 2001; Wulff et al. 2001a, 2001b; Fraser et al. 2005), also implying changes in permeability. Again, this has not been visualized in real time over the period of change. From a practical viewpoint, the experiments present a challenge in terms of stability of physiological as well as image parameters. Because the animals are under anesthesia for a long period, hemodynamic parameters such as blood pressure and cardiac output, as well as CL tissue status including humidity and temperature control, should be incorporated in the experimental design.

Finally, the ovarian sheep model, apart from a microvascular model, is the most useful for reproductive sciences' knowledge transfer to human studies because: (i) it is mono-ovular; (ii) the control of ovarian function is very similar to the human, in numbers of follicles activated and time to preovulatory follicle formation; (iii) the gonadotrophic control of ovarian activity is almost identical to the human; (iv) imaging with ultrasound is suited to the tissue and is similar to the human; and (v) wide knowledge and expertise are available to manipulate ovarian function, particularly the CL. Disease prevention coupled with early diagnosis and intervention are crucial in the female reproductive system and an imaging tool

useful in a number of conditions that present changes in microvascularity may be developed further from this research. Currently, there is no reliable noninvasive tool for diagnosis and monitoring of endometriosis (Girling and Rogers 2005; Jones et al. 2006), adenomyosis (Ross 2001; Dueholm et al. 2001) and ectopic pregnancy (Duncan et al. 1995; Farquhar 2005; Horne et al. 2008). The assessment of microvascular perfusion during transvaginal sonography would represent a major clinical advance toward addressing those problems. Also, it appears that the current criteria for polycystic ovary syndrome identify more than one phenotype for the disease (Porter 2008), and an improvement of microvascular assessment of the ovary may help redefine and standardize these criteria. Considering that ultrasound imaging is a major diagnostic tool in obstetrics and gynecology and CEUS is a safe noninvasive technique (Main et al. 2009), the applications just proposed here are very attractive.

CONCLUSIONS

The accurate assessment of microvascular blood flow and volume is one of the goals of ultrasound contrast imaging. Although various clinical applications have recently appeared in the clinic, and the applicability of the field is expanding, an *in vivo* model is required for the improvement of microvascular measurements. The ovine CL is proposed here as such a model. The image results were reproducible using a linear array and low MI imaging, and thus detailed quantification of the intensity is possible. The low uncertainty, $<10\%$, of the WIT and the excellent agreement with histological data showed that small microvascular changes of the CL are possible to measure with CEUS. In addition, the feasibility of a vascular regulation measurement was demonstrated.

Acknowledgments—The authors wish to express their gratitude to Sarah Henderson for immunohistochemistry. The work was funded by Dr. Sboros BHF fellowship (FS/07/052), UK MRC project grant G0800896 and UK MRC support to Professor McNeilly (G7 002.00007.01).

REFERENCES

Arditi M, Frinking PJA, Zhou X, Rognin NG. A new formalism for the quantification of tissue perfusion by the destruction-replenishment method in contrast ultrasound imaging. IEEE Trans Ultrason Ferroelectr Freq Control 2006;53:1118–1229.

Averkiou M, Lampaskis M, Kyriakopoulou K, Skarlos D, Klouvas G, Strouthos C, Leen E. Quantification of tumor microvascularity with respiratory gated contrast-enhanced ultrasound for monitoring therapy. Ultrasound Med Biol 2010;36:68–77.

Baird DT, McNeilly AS. Gonadotrophic control of follicular development and function during the oestrous cycle of the ewe. J Reprod Fertil 1981;Sl30:119–133.

Baird DT, Swanston IA, McNeilly AS. Relationship between LH, FSH, and prolactin concentration and the secretion of androgens and estrogens by the preovulatory follicle in the ewe. Biol Reprod 1981;24:1013–1025.

Correas JM, Tranquart MCF, Helenon O. The kidney: Imaging with microbubble contrast agents. Ultrasound Q 2006;22:53–66.

Dickson SE, Bicknell R, Fraser HM. Mid-luteal angiogenesis and function in the primate is dependent on VEGF. J Endocrinol 2001;168: 409–416.

Dueholm M, Lundorf E, Hansen ES, Sørensen JS, Ledertoug S, Olesen F. Magnetic resonance imaging and transvaginal ultrasonography for the diagnosis of adenomyosis. Fertil Steril 2001;76: 588–594.

Duncan WC, Sweeting VM, Cawood P, Illingworth PJ. Measurement of creatine-kinase activity and diagnosis of ectopic pregnancy. Br J Obstet Gynecol 1995;102:233–237.

Farquhar CM. Ectopic pregnancy. Lancet 2005;366:583–591.

Fisher NG, Christiansen PC, Leong-Poi H, Jayaweera AR, Lidner JR, Kaul S. Myocardial and microcirculatory kinetics of BR14, a novel third-generation intravenous ultrasound contrast agent. J Am Coll Cardiol 2002;39:530–537.

Fraser HM, Lunn SF. Angiogenesis and its control in the female reproductive system. Br Med Bull 2000;56:787–797.

Fraser HM, Dickson SE, Lunn SF, Wulff C, Morris KD, Carroll V, Bicknell R. Suppression of luteal angiogenesis in the primate after neutralization of vascular endothelial growth factor. Endocrinology 2000;141:995–1000.

Fraser HM, Wilson H, Rudge JS, Wiegand SJ. Single injections of vascular endothelial growth factor trap block ovulation in the macaque and produce a prolonged, dose-related suppression of ovarian function. J Clin Endocrinol Metab 2005;90:1114–1122.

Fraser HM, Duncan WC. Regulation and manipulation of angiogenesis in the ovary and endometrium. Reprod Fertil Dev 2009;21:377–392.

Girling JE, Rogers PA. Recent advances in endometrial angiogenesis research. Angiogenesis 2005;8:89–99.

Gudmundsson P, Shahgaldi K, Winter R, Dencker M, Kitlinski M, Thorsson O, Ljunggren L, Willenheimer R. Parametric quantification of myocardial ischaemia using real-time perfusion adenosine stress echocardiography images, with SPECT as reference method. Clin Physiol Funct Imaging 2010;30:30–42.

Horne AW, van den Driesche S, King AE, Burgess S, Myers M, Ludlow H, Lourenco P, Ghazal P, Williams AR, Critchley HO, Duncan WC. Endometrial inhibin/activin beta-B subunit expression is related to decidualization and is reduced in tubal ectopic pregnancy. J Clin Endocrinol Metab 2008;93:2375–2382.

Jayaweera AR, Edwards N, Glasheen WP, Villanueva FS, Abbott RD, Kaul S. In vivo myocardial kinetics of air-filled albumin microbubbles during myocardial contrast eecchocardiography. Comparison with radiolabeled red blood cells. Circ Res 1994;74:1157–1165.

Jones G, Jenkinson C, Taylor N, Mills A, Kennedy S. Measuring quality of life in women with endometriosis: Tests of data quality, score reliability, response rate and scaling assumptions of the Endometriosis Health Profile Questionnaire. Hum Reprod 2006;21:2686–2693.

Kaufmann BA, Wei K, Lindner JR. Contrast echocardiography. Curr Probl Cardiol 2007;32:51–96.

Klibanov AL, Rasche PT, Hughes MS, Wojdyla JK, Galen KP, Wible JH, Brandenburger GH. Detection of individual microbubbles of an ultrasound contrast agent: Fundamental and pulse inversion imaging. Acad Radiol 2002;9:S279–S281.

Kohzuki M, Kanzaki T, Murata Y. Contrast-enhanced power Doppler sonography of malignant ovarian tumors using harmonic flash-echo imaging: Preliminary experience. J Clin Ultrasound 2005;33: 237–242.

Lampaskis M, Kyriakopoulou K, Skarlos D, Klouvas G, Strouthos C, Leen E, Averkiou M. Quantification of tumor microvascularity with respiratory gated contrast enhanced ultrasound for monitoring therapy. Ultrasound Med Biol 2010;36:306–312.

Lassau N, Chami L, Benatsou B, Peronneau P, Roche A. Dynamic contrast-enhanced ultrasonography (DCE-US) with quantification of tumor perfusion: A new diagnostic tool to evaluate the early effects of antiangiogenic treatment. Eur Radiol Suppl 2007;17 (Suppl 6):F89–F98.

Lindner JR, Song J, Jayaweera AR, Sklenar J, Kaul S. Microvascular rheology of Definity microbubbles after intra-arterial and intravenous administration. J Am Soc Echocardiogr 2002;15:396–403.

Main ML, Goldman JH, Grayburn PA. Ultrasound contrast agents: Balancing safety versus efficacy. Exp Op Dr Safety 2009;8:49–56.

Marret H, Brewer M, Giraudeau B, Tranquart F, Satterfield W. Assessment of cyclic changes of microvessels in ovine ovaries using SonoVue contrast-enhanced ultrasound. Ultrasound Med Biol 2006;32: 163–169.

McNeilly AS, Fraser HM. Effect of gonadotrophin-releasing hormone agonist-induced suppression of LH and FSH on follicle growth and corpus luteum function in the ewe. J Endocrinol 1987;115: 273–282.

McNeilly AS, Crow WJ, Fraser HM. Suppression of pulsatile luteinizing hormone secretion by gonadotrophin-releasing hormone antagonist does not affect episodic progesterone secretion or corpus luteum function in ewes. J Reprod Fertil 1992a;96:865–874.

McNeilly AS, Crow W, Brooks J, Evans G. Luteinizing hormone pulses, follicle-stimulating hormone and control of follicle selection in sheep. J Reprod Fertil 1992b;99:5–19.

Ohtani M, Takase S, Wijayagunawardane MPB, Tetsuka M, Miyamoto A. Reprod 2004;127:117–124.

Orden MR, Jurvellin JS, Kirkinen PP. Kinetics of a US contrast agent in benign and malignant adnexal tumors. Radiology 2003;226: 405–410.

Quaia E. Microbubble ultrasound contrast agents: An update. Eur Radiol 2007;17:1995–2008.

Porter MB. Polycystic ovary syndrome: The controversy of diagnosis by ultrasound. Sem Reprod Med 2008;26:241–251.

Redmer DA, Doraiswamy V, Bortmen BJ, Fisher K, Joblonka-Shariff A, Grazul-Bilska AT, Reynolds LP. Evidence for a role of capillary pericytes in vascular growth of the developing ovine corpus luteum. Biol Reprod 2001;65:879–889.

Ross J. Extracts from "Clinical Evidence"—pelvic inflammatory disease. BMJ 2001;322:658–659.

Sboros V, Moran CM, Anderson T, Pye SD, Macleod IC, Millar AM, McDicken WN. Evaluation of an experimental system for the in-vitro assessment of ultrasonic contrast agents. Ultrasound Med Biol 2000;26:105–111.

Sboros V, Moran CM, Pye SD, McDicken WN. Contrast agent stability: A continuous B-mode imaging approach. Ultrasound Med Biol 2001;27:1367–1377.

Sboros V, MacDonald CA, Pye SD, Moran CM, Gomatam J, McDicken WN. The dependence of ultrasound contrast agents backscatter on acoustic pressure: Theory versus experiment. Ultrasonics 2002a;40:579–583.

Sboros V, Ramnarine KV, Moran CM, Pye SD, McDicken WN. Understanding the limitations of ultrasonic backscatter measurements from microbubble populations. Phys Med Biol 2002b;47: 4287–4299.

Sboros V, Moran CM, Pye SD, McDicken WN. The behaviour of individual contrast agent microbubbles. Ultrasound Med Biol 2003;29: 687–694.

Sboros V, Tang M-X. The assessment of microvascular flow and tissue perfusion using ultrasound imaging. J Eng Med 2010;224(H2): 273–290.

Souza CJH, Campbell BK, McNeilly AS, Baird DT. What the known phenotypes of the Booroola mutation can teach us about its mechanism of action. Reprod Suppl 2003;61:361–370.

Souza CH, Campbell BK, McNeilly AS, Baird DT. Mechanisms of action of the principal prolific genes and their application to sheep production. Reprod Fertil Dev 2004;16:395–401.

Strouthos C, Lampaskis M, Sboros V, McNeilly A, Averkiou M. Indicator dilution models for the quantification of microvascular blood flow with bolus administration of ultrasound contrast agents. IEEE Trans Ultrason Ferroelectr Freq Control 2010;57:1296–1310.

Talu E, Powell RL, Longo ML, Dayton PA. Needle size and injection rate impact microbubble contrast agent population. Ultrasound Med Biol 2008;34:1182–1187.

Tang M-X, Eckersley RJ, Noble JA. Pressure-dependent attenuation with microbubbles at low mechanical index. Ultrasound Med Biol 2005;31:377–384.

Tang M-X, Eckersley RJ. Nonlinear propagation of ultrasound through microbubble contrast agents and implications for imaging. IEEE Trans Ultrason Ferroelectr Freq Control 2006;53:2406–2415.

Tang M-X, Eckersley RJ. Frequency and pressure dependent attenuation and scattering by microbubbles. Ultrasound Med Biol 2007;33: 164–168.

Testa AC, Timmerman D, Exacoustos C, Fruscella E, Van Holsbeke C, Bokor D, Arduini D, Scambia G, Ferrandina G. The role of CnTI-SonoVue in the diagnosis of ovarian masses with papillary projections: a preliminary study. Ultrasound Obstet Gynecol 2007;29: 512–516.

Thomas DH, Butler MB, Anderson T, Steel R, Pye SD, Poland M, Brock-Fisher T, McDicken WN, Sboros V. Single microbubble response using pulse sequences: Initial results. Ultrasound Med Biol 2009a;35:112–119.

Thomas DH, Looney P, Steel R, Pelekasis N, McDicken WN, Anderson T, Sboros V. Acoustic detection of microbubble resonance. Appl Phys Lett 2009b;94:243902.

Vonnahme KA, Redmer DA, Borowczyk E, ilski JJ, Luther JS, Johnson ML, Reynolds LP, Grazul-Bilska AT. Vascular composition, apoptosis, and expression of angiogenic factors in the corpus luteum during prostaglandin F2alpha-induced regression in sheep. Reproduction 2006;131:1115–1126.

Wulff C, Wilson H, Rudge JS, Wiegand SJ, Lunn SF, Fraser HM. Luteal angiogenesis: Prevention and intervention by treatment with vascular endothelial growth factor trap A40. J Clin Endocrinol Metab 2001a;87:3377–3386.

Wulff C, Weigand SJ, Saunders PTK, Scobie GA, Fraser HM. Angiogenesis during follicular development in the primate and its inhibition by treatment with truncated Flt-1-Fc (vascular endothelial growth factor Trap A40). Endocrinology 2001b;142:3244–3254.

Wulff C, Wilson H, Wiegand SJ, Rudge JS, Fraser HM. Prevention of thecal angiogenesis, antral follicular growth, and ovulation in the primate by treatment with vascular endothelial growth factor trap R1R2. Endocrinology 2002;143:2797–2807.

Yong P, Baird DT, Thong J, McNeilly AS, Anderson RA. Prospective analysis of the relationships between the ovarian follicle cohort and basal FSH concentration, the inhibin response to exogenous FSH, ovarian follicle number at different stages of the normal menstrual cycle and after pituitary down-regulation. Hum Reprod 2003;18:35–44.